



Investigating the fragmentation of charm quarks with correlation and jet measurements by ALICE

Ravindra Singh **on behalf of the ALICE Collaboration**
Indian Institute of Technology Indore (IN)

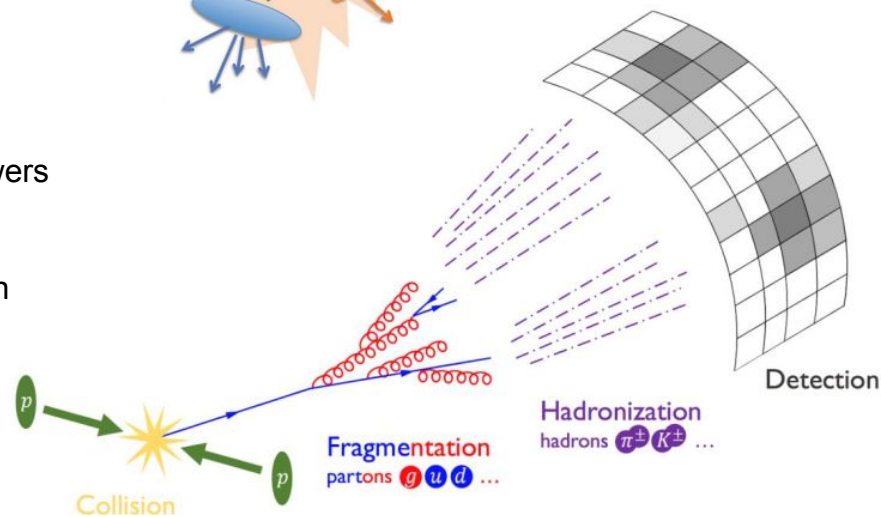
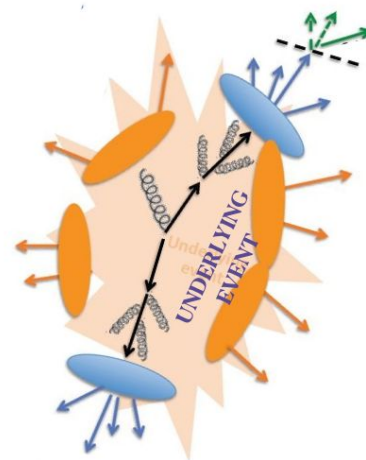
DAE-HEP2022, 12-16 Dec 2022

Why heavy-flavour jets?

- Heavy-Flavours
 - Heavy-flavour jets minimize dependence on hadronization process due to including all particles from parton shower.

What do we learn by investigating different systems?

- **pp collisions**
 - Test for pQCD calculations
 - Investigate fragmentation and hadronization models
 - Mass dependence of parton radiation
 - Differences between quark-initiated and gluon initiated showers
- **p-Pb Collisions**
 - Modification due to Cold Nuclear Matter (CNM) effects, gluon saturation effect.
- **Pb-Pb collisions**
 - Modification due to the interaction with the Quark Gluon Plasma (QGP), such as energy loss mechanisms.

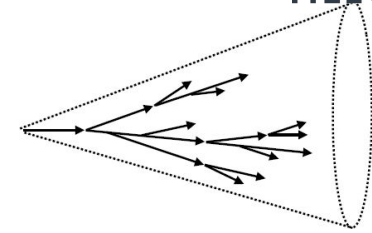


How the jets can help?

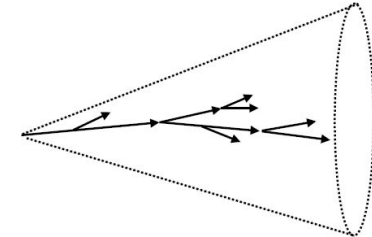
- Smaller dependence on the hadronization models allows for a better comparison to QCD.
 - **Gluon initiated jets** – broader fragmentation
 - Quark initiated jets – more collimated
- **Inclusive jets**
 - Well constrained at high p_T , low p_T experimentally challenging.
 - Mostly gluon initiated.
- **Heavy-flavour jets:**
 - Heavy quarks are conserved through the parton shower
 - Quark initiated
- Inclusive vs heavy-flavour jets
 - Effect of Casimir factors and dead cone

$$C_A/C_F = 9/4$$

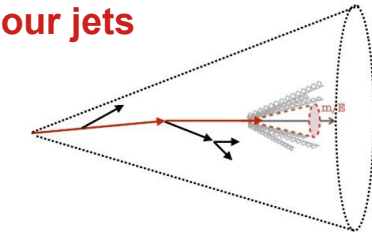
Gluon initiated jets



Quark jets



Heavy-flavour jets



Heavy-flavour (HF) correlation

- HF correlations represents an alternative method to study the HF parton shower.

Advantage over jet:

- Better access to low p_T parton showers
- Description of peak shapes and width
- Give access to the production mechanisms:

- Pair Creation (LO):

- quarks are produced back-to-back
- “Near Side” peak at $\Delta\varphi = 0$: Produced by the particle associated with high p_T trigger particle.
- “Away side” peak at $\Delta\varphi = \pi$: Produced by the particles associated with the recoiled jet.

- Hard gluon radiation (NLO):

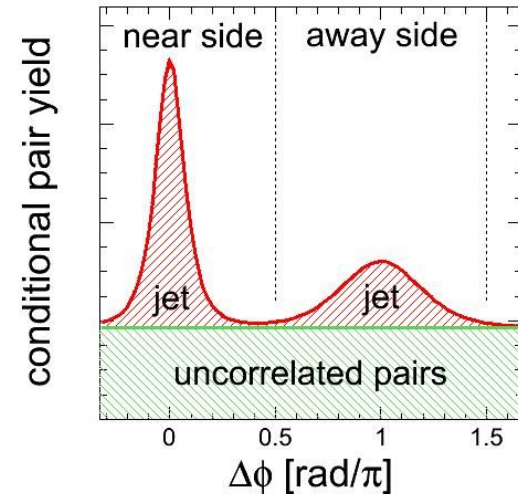
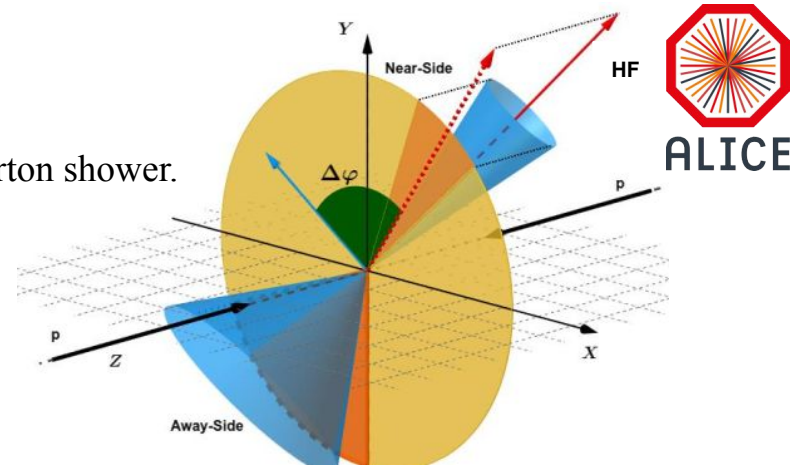
- Broadening of both peaks

- Gluon splitting (NLO):

- Heavy-flavours are produced close in phase space

- Flavour excitation (NLO):

- Flat $\Delta\varphi$ contribution.



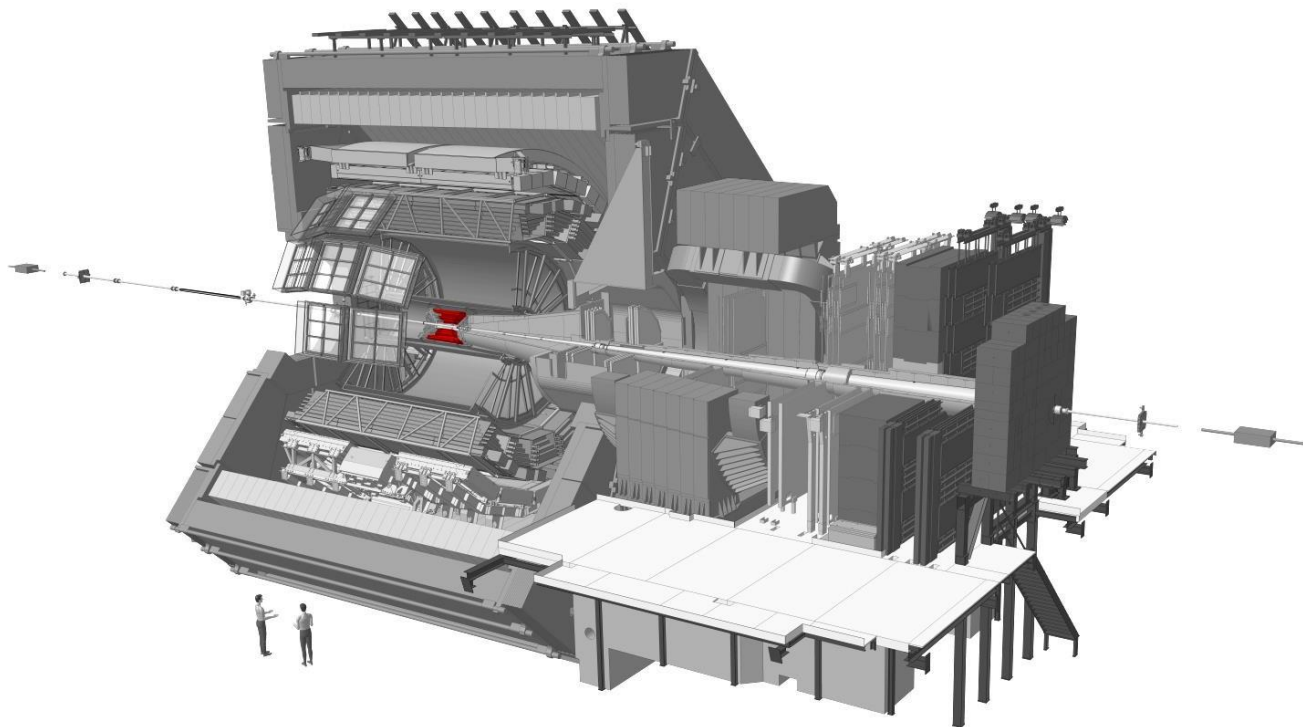
The ALICE Detector – Inner Tracking System



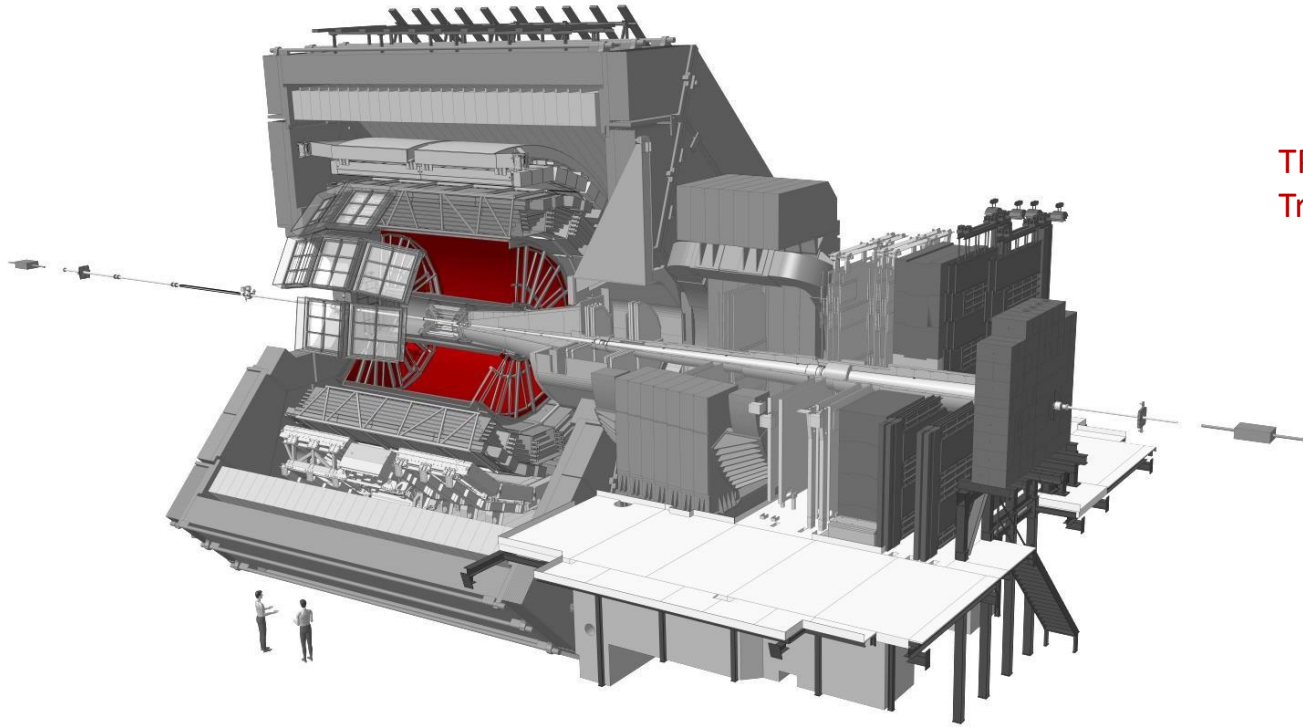
Detectors

ITS $|\eta| < 0.9$

Vertexing and tracking

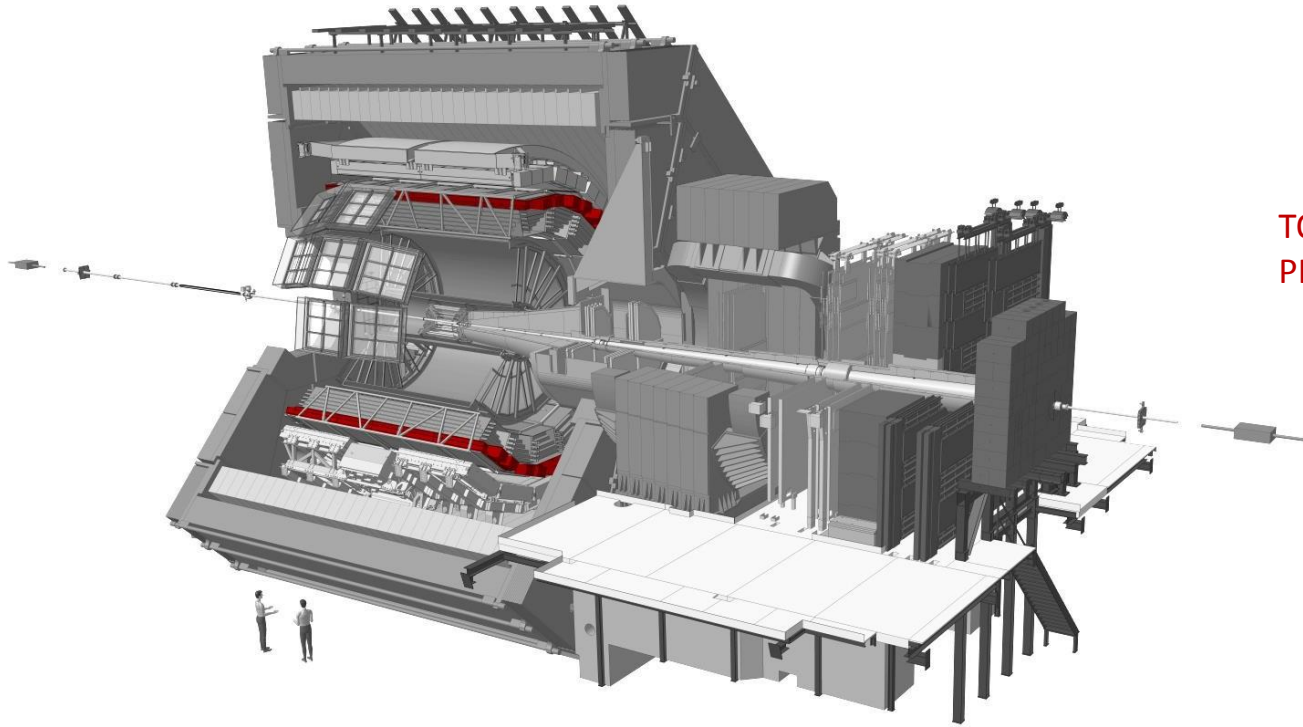


The ALICE Detector (Time Projection Chamber)



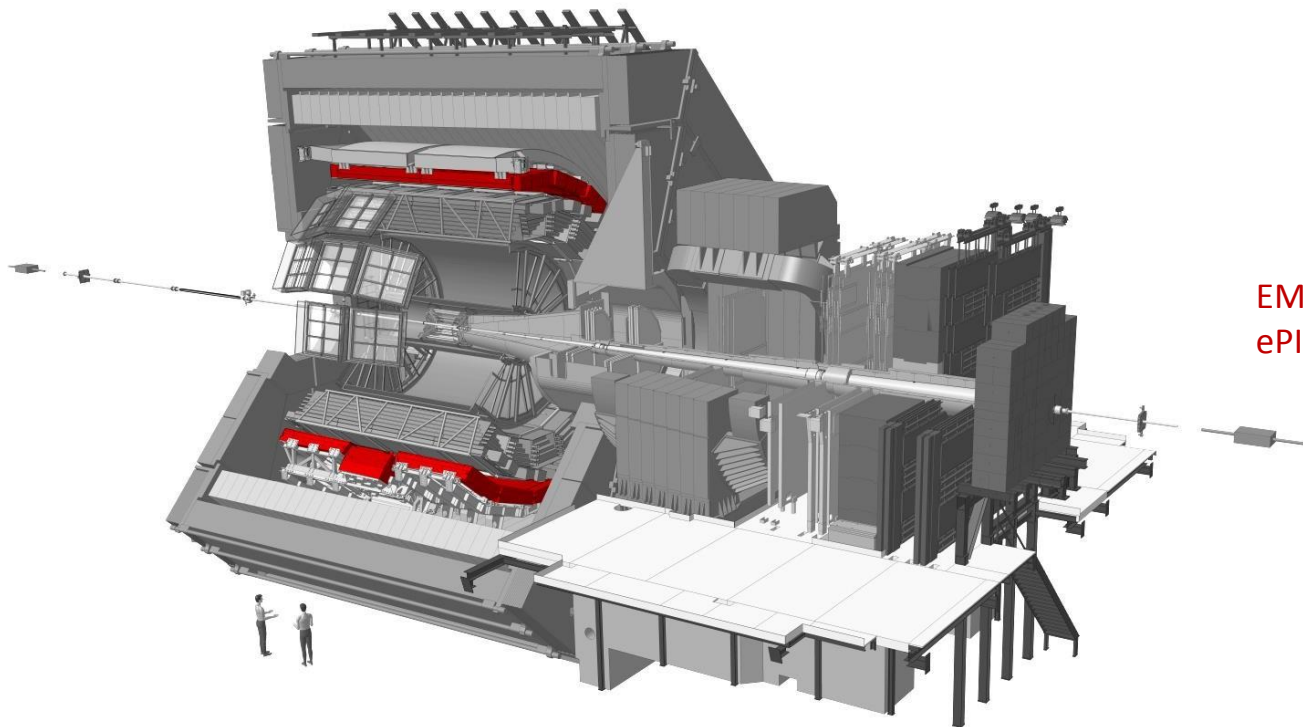
TPC $|\eta| < 0.9$
Tracking and PID

The ALICE Detector – Time of Flight



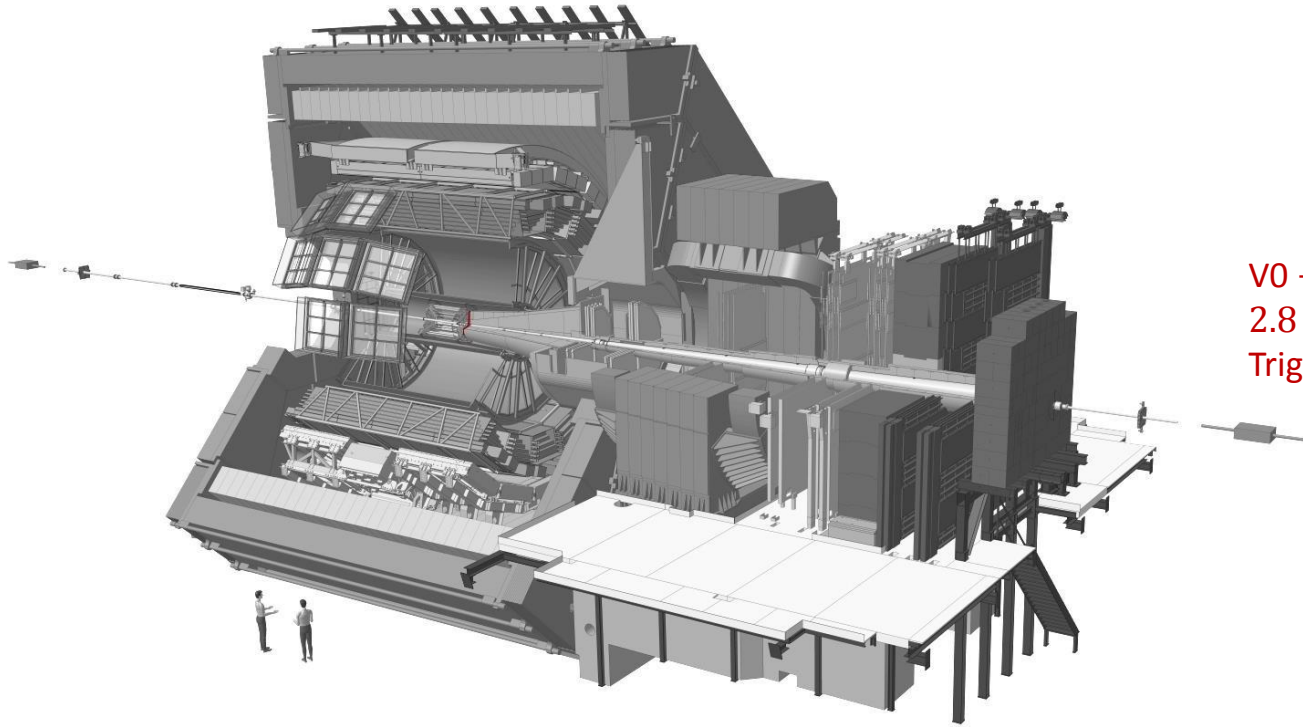
TOF $|\eta| < 0.9$
PID

The ALICE Detector – Calorimeters



EMCAL/PHOS $|\eta| < 0.7$
ePID and trigger

The ALICE Detector – V0



V0 $-3.7 < \eta < -1.7$

$2.8 < \eta < 5.1$

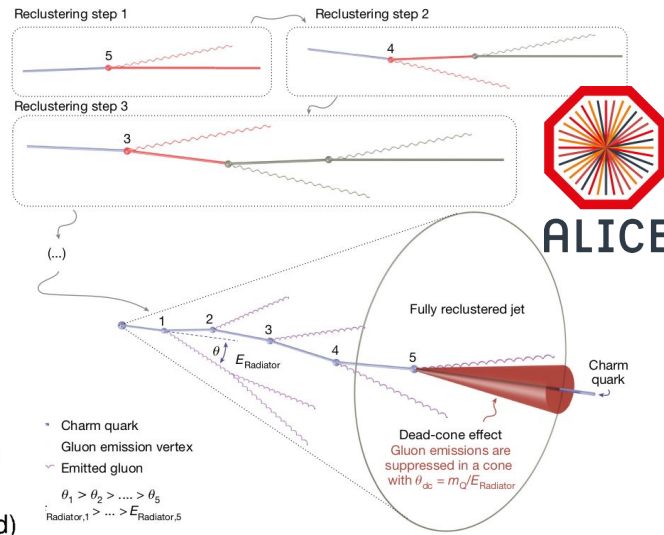
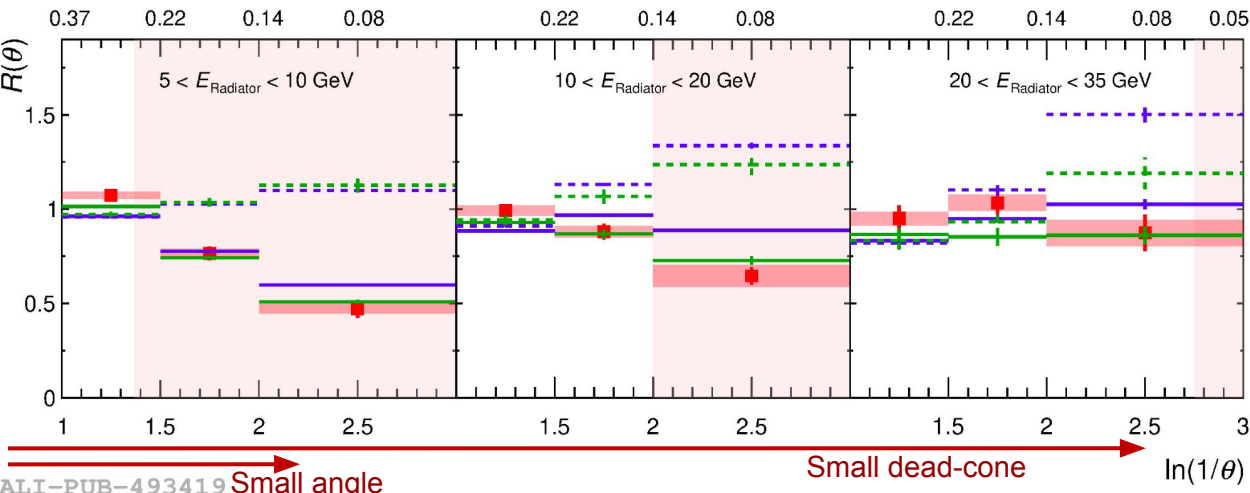
Trigger and background rejection

Dead-cone effect

- The dead-cone (DC) effect is a fundamental feature of all gauge field theories
- The radiation of the emitter is suppressed for $\theta < \theta_{DC} = \frac{m_q}{E_q}$

Mass $\uparrow \rightarrow \theta_{DC} \uparrow \rightarrow$ collinear radiation \downarrow

■ ALICE Data --- PYTHIA 8 LQ / inclusive no dead-cone limit $pp \sqrt{s} = 13 \text{ TeV}$
— PYTHIA 8 $\text{charged jets, anti-}k_T, R=0.4$ $p_{T, \text{inclusive jet}}^{\text{ch, leading track}} \geq 2.8 \text{ GeV}/c$
— SHERPA --- SHERPA LQ / inclusive no dead-cone limit $k_T > \Lambda_{\text{QCD}}, \Lambda_{\text{QCD}} = 200 \text{ MeV}/c$
 C/A reclustering $|\eta_{\text{lab}}| < 0.5$ $\theta \text{ (rad)}$



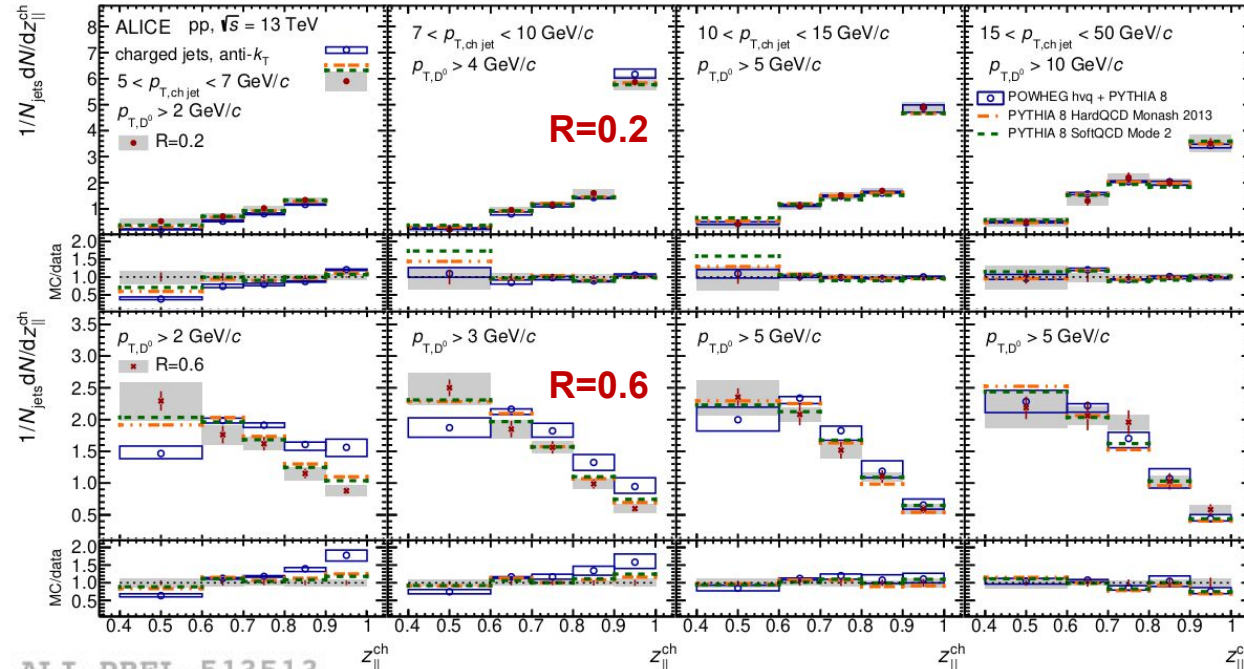
D^0 reconstruction \rightarrow C/A algorithm
 \rightarrow angular-ordered splitting tree
 Unwind the charm shower process $\rightarrow (E_{\text{rad}}, \theta)$

$$R(\theta) = \frac{1}{N^{D^0 \text{ jets}}} \frac{dn^{D^0 \text{ jets}}}{d \ln(1/\theta)} / \frac{1}{N^{\text{inclusive jets}}} \frac{dn^{\text{inclusive jets}}}{d \ln(1/\theta)} \Bigg|_{k_T, E_{\text{Radiator}}}$$

- \rightarrow Suppression for D^u -meson tagged jets
- \rightarrow Dependency on E_{rad} of the suppression

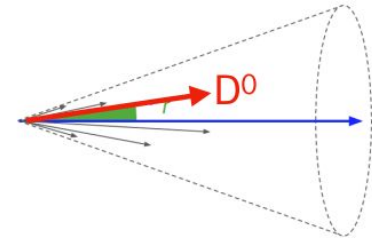
[ALICE, Nature 605 \(2022\)](#)

HF jets to look into fragmentation



Provide access to the properties of heavy-quarks fragmentation and hadronization

$$Z_{||}^{ch} = \frac{\vec{p}_{ch jet} \cdot \vec{p}_{HF}}{\vec{p}_{ch jet} \cdot \vec{p}_{ch jet}}$$



ALI-PREL-513513

<https://doi.org/10.48550/arXiv.2204.10167>

- Hint of a softer fragmentation in data with respect to model predictions (especially NLO) for low $p_{T, ch jet}$ and large R .
- The core of the jet ($R=0.2$) is dominated by the HF hadron, as expected from the suppression of small angle emissions.
- At large angle ($R>0.2$) the charm quark emissions are recovered.

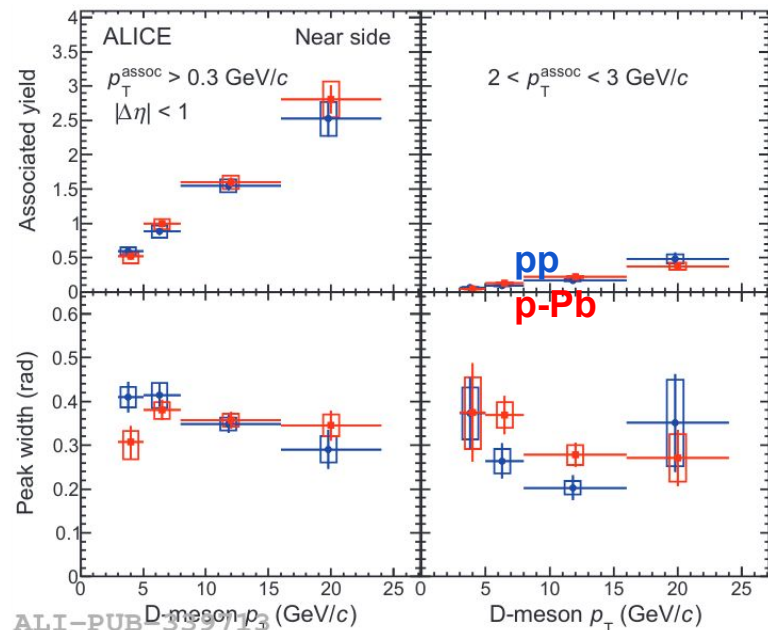
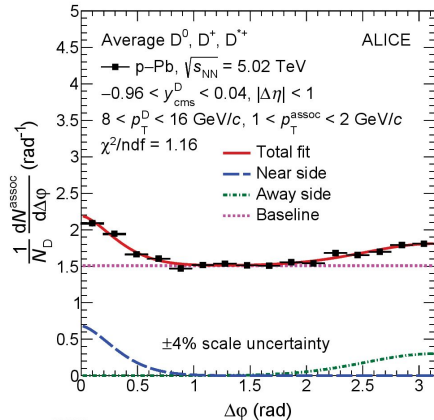
D-meson and charged particle azimuthal correlation

- **Yield**: indication of charm-shower multiplicity
- **Width**: angular distribution of charm-shower

Fitting procedure:

- constant term (Baseline) + Generalized Gaussian (Near-side) + Gaussian (Away-side)

$$f(\Delta\varphi) = b + \frac{Y_{NS} \times \beta}{2\alpha\Gamma(1/\beta)} \times e^{-\left(\frac{\Delta\varphi}{\alpha}\right)^\beta} + \frac{Y_{AS}}{\sqrt{2\pi}\sigma_{AS}} \times e^{-\frac{(\Delta\varphi-\pi)^2}{2\sigma_{AS}^2}}$$



ALI-PUB-339713

$p_T^D \uparrow$ Yield \uparrow Width \downarrow

[EPJC 80 \(2020\) 979](#)

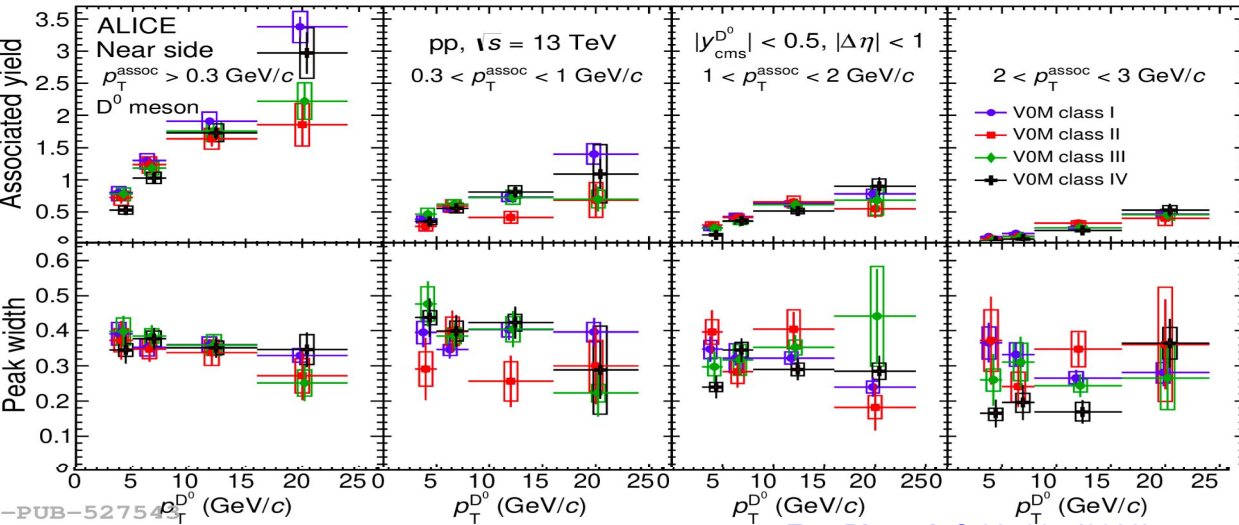
- Consistent values of the near-side observables in pp and p-Pb collisions are observed for all kinematic ranges.
- no significant impact from cold-nuclear-matter effects on the charm fragmentation is observed with current statistics.



ALICE

D-meson and charged particle azimuthal correlation

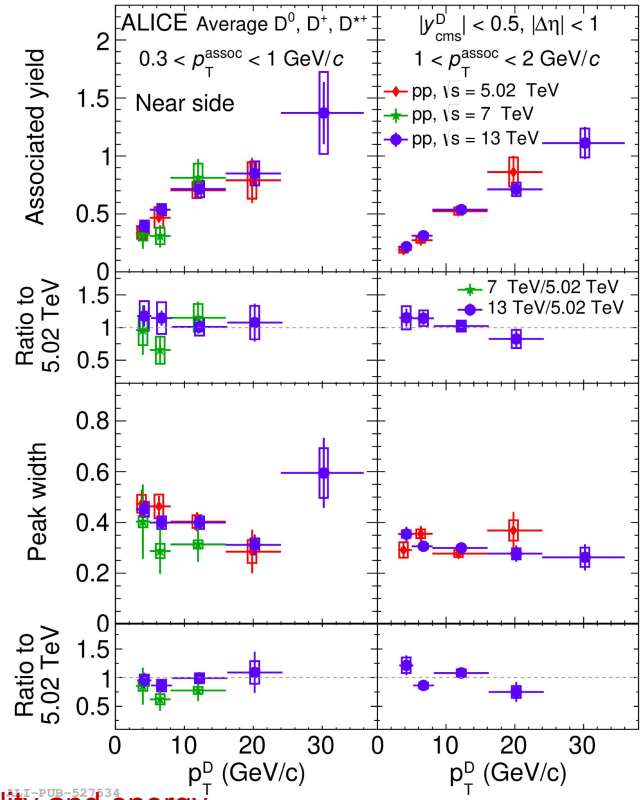
Comparison with different centrality classes and collision energies



[Eur. Phys. J. C 82, 335 \(2022\)](#)

VOM multiplicity class	I	II	III	IV
$\sigma/\sigma_{\text{INEL}>0}$ (%)	0–0.0915	0.0915–9.149	9.149–27.50	27.50–100
$\langle dN_{\text{ch}}/d\eta \rangle$	31.15 ± 0.40	18.39 ± 0.23	11.46 ± 0.15	4.41 ± 0.06

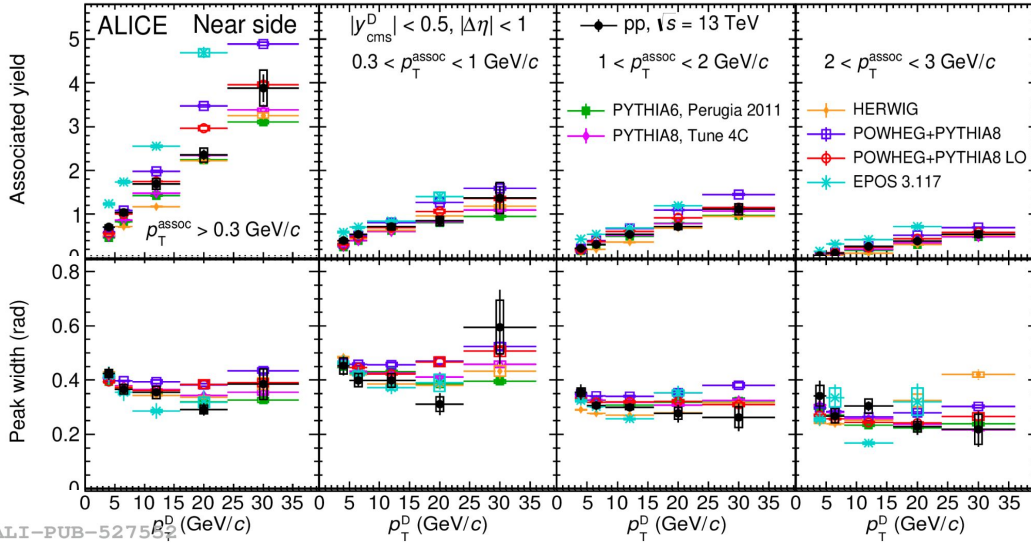
- An increasing trend is observed with p_{T}^{D} .
- Charm fragmentation and hadronization show no dependence on collision centrality and energy.



[PUB-527634](#)

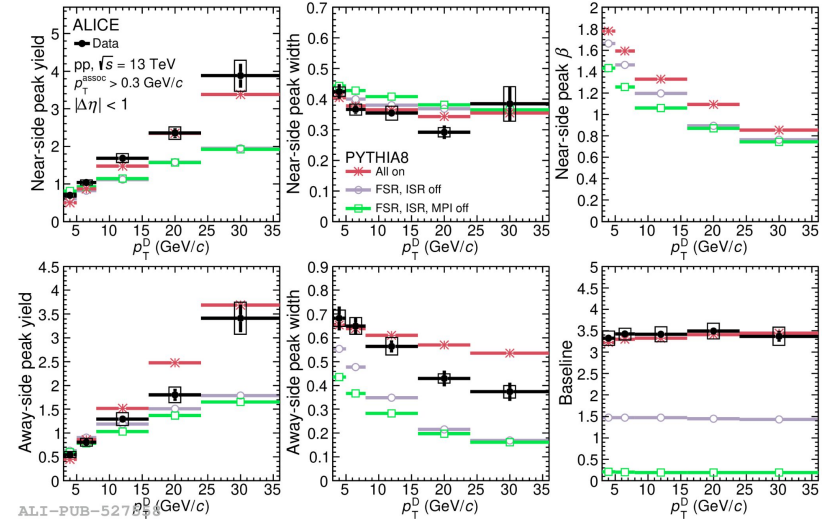
D-meson and charged particle azimuthal correlation

Comparison with different models and investigation of partonic processes



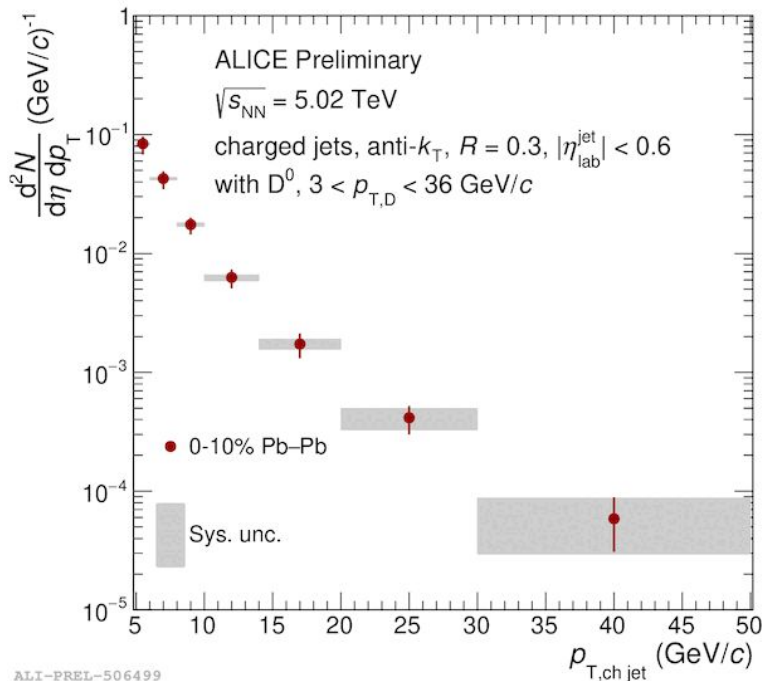
From the comparison with MonteCarlo predictions, **PYTHIA** and **POWHEG+PYTHIA** provide the best description

[Eur. Phys. J. C 82, 335 \(2022\)](#)

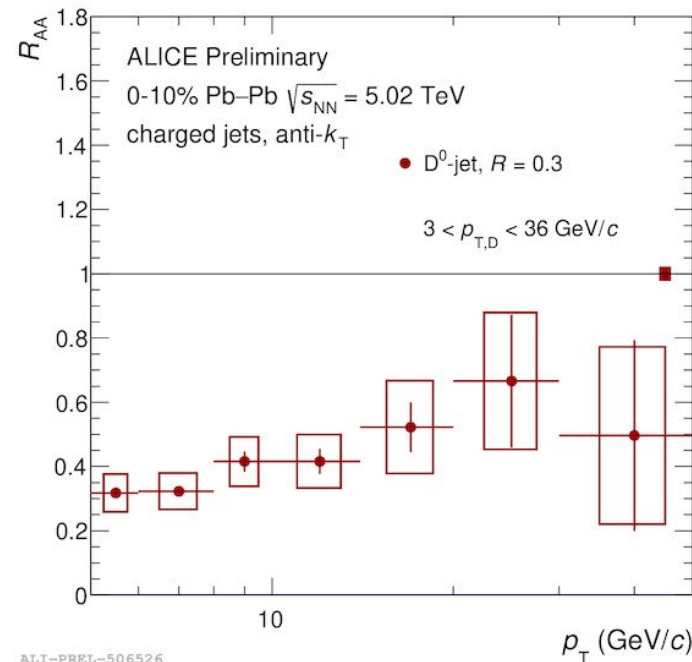


Multi-partonic interaction (MPI) → No change in yields
 (Contribute to underlying events)
 Initial- and final-state radiation processes → increase peak yields
 (additional production of collinear particles)
 All partonic processes → increase widths
 (Presence of hard gluons)

Medium effects: D^0 -jets in 0-10% Pb-Pb



p_T -differential cross section in Pb-Pb central collisions

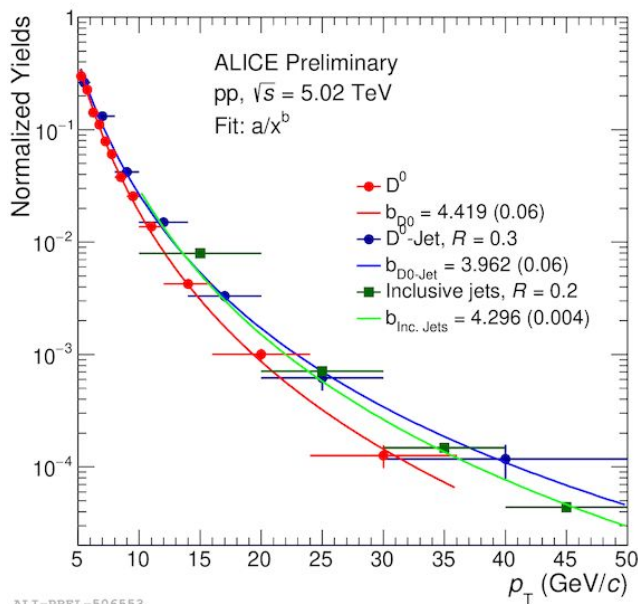


- Baseline: D^0 -jet p_T differential cross section in pp at 5.02 TeV with same jet reconstruction as in Pb-Pb.
- An area based background subtraction performed in Pb-Pb.

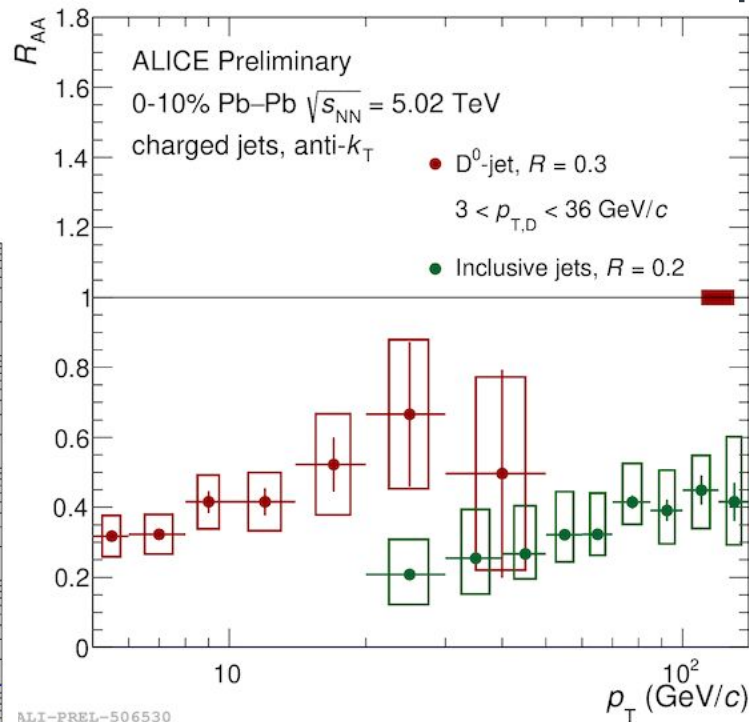
Sizeable suppression of D^0 -jets in central Pb-Pb collisions

Medium effects: D^0 -jets in 0-10% Pb-Pb

- Higher R_{AA} of D^0 -jet compared to inclusive jets in Pb-Pb?
- Comparison is sensitive to difference between quarks and gluon energy loss (Casimir colour effect)
- Comparison could also be sensitive to mass effects (dead-cone).



ALI-PREL-506553



ALI-PREL-506530

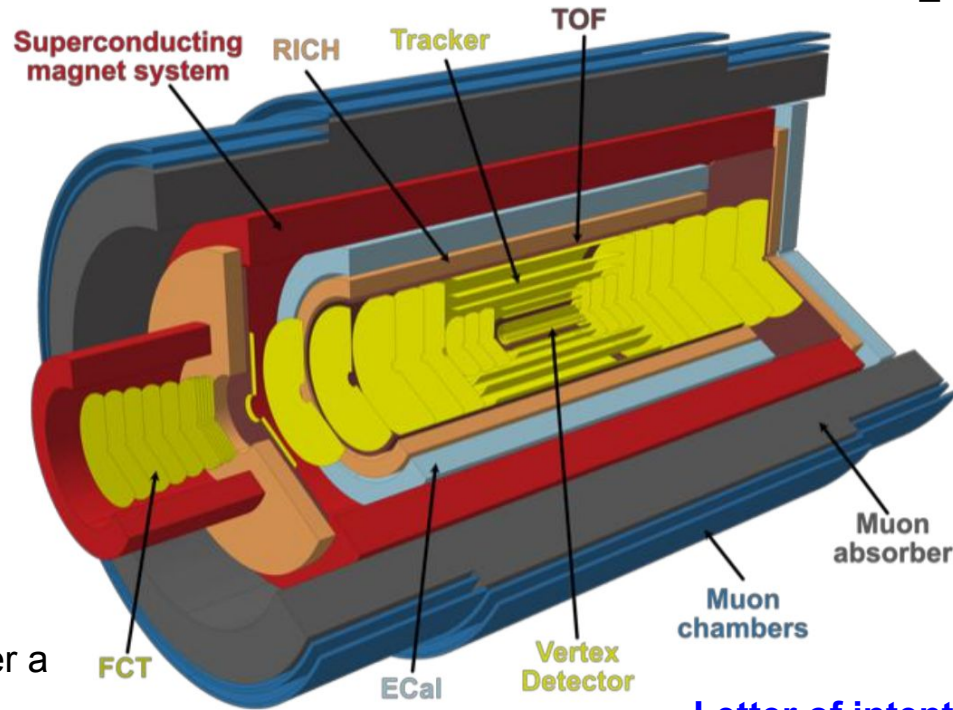
ALICE 3 Detector

- ALICE 3: a next-generation heavy-ion experiment for LHC Run 5 and 6.
- Compact all-silicon tracker with high-resolution vertex detector.



ALICE

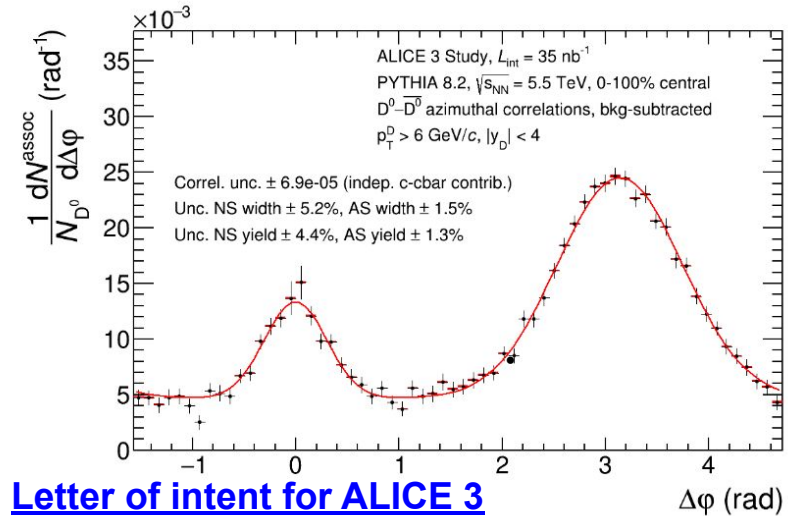
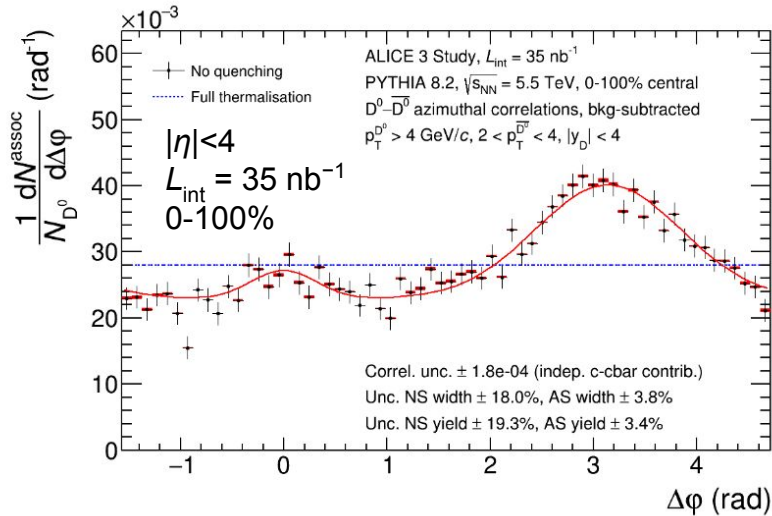
Heavy-flavour hadrons
($p_T \rightarrow 0$, wide η range)
– vertexing, tracking, hadron ID



Particle identification over a large acceptance.

[Letter of intent for ALICE 3](#)

Expected performance of D^0 - \bar{D}^0 azimuthal correlation in Pb-Pb collisions



[Letter of intent for ALICE 3](#)

- Includes background subtraction and weights to account for D^0 - \bar{D}^0 reconstruction and selection efficiencies. Normalization to the number of trigger D^0 mesons.
- Correlation patterns in Pb-Pb collisions will be accurate enough to assess the effects of in-medium broadening and thermalisation, using pp collisions as a reference.

Summary:

- **HF - tagged jets:**

- ✓ Softer fragmentation at low $p_{T, \text{ch jet}}$ is observed by looking at the fragmentation function.
- ✓ Nuclear modification factor in D-meson tagged jets shows suppression up to 70%.

- **D-h azimuthal correlation distribution:**

- ✓ Comparison between pp and p-Pb measurements showing consistency with each other.
- ✓ No significant modifications were observed due to the CNM effect.
- ✓ Jet-fragmentation dependency on multiplicity and collision energy not observed.
- ✓ PYTHIA and POWHEG+PYTHIA provide the best description of data.

- **ALICE3 Detector**

- ✓ Wide η range
- ✓ Correlation patterns in Pb-Pb collisions will be accurate enough to assess the effects of in-medium broadening and thermalisation.

*Thank
you*



Back-up slides

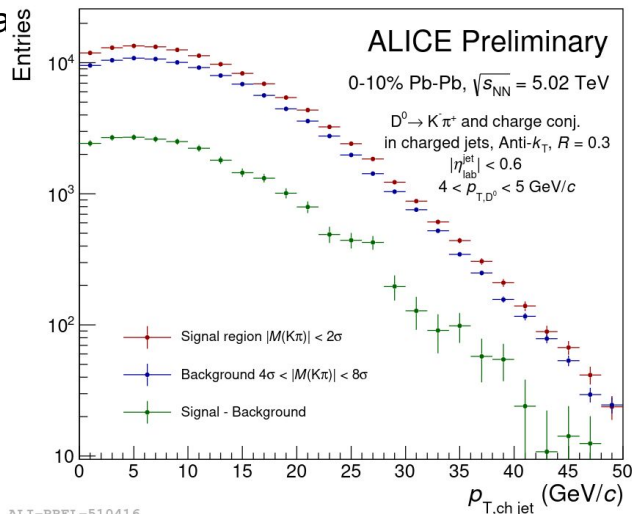
Medium effects: D^0 -jets in 0-10% Pb-Pb

- Invariant mass was used to extract D^0 -jet raw signal spectrum with side-band subtraction.
- Correction for the D^0 -jet efficiency and D^0 -reflections.
- Subtraction of feed-down D^0 -jet component.
- POWHEG predictions convoluted with measured non-prompt D^0

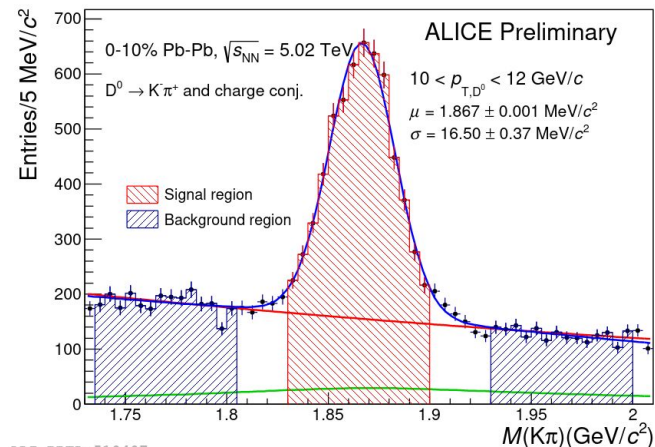
R_{AA}

- Jet- p_T spectra corrected for detector effects and background fluctuations
- Unfolding using an itera

Raw jet spectrum corrected for D^0 -jet efficiency



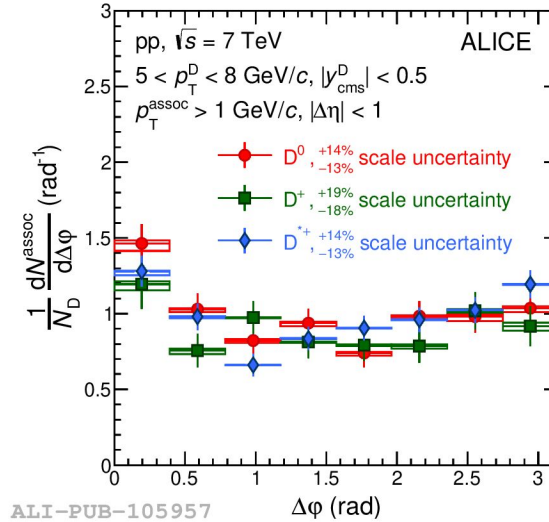
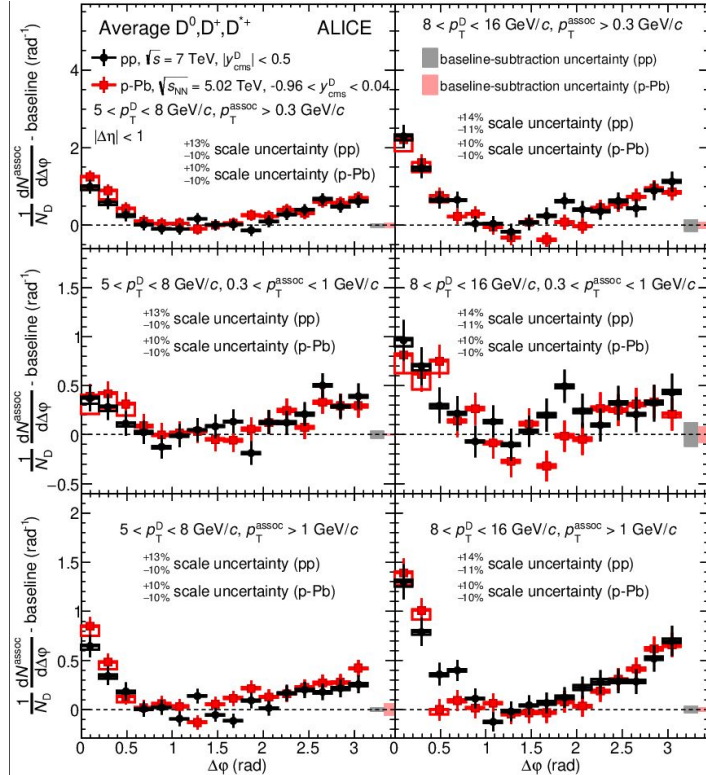
ALI-PREL-510416



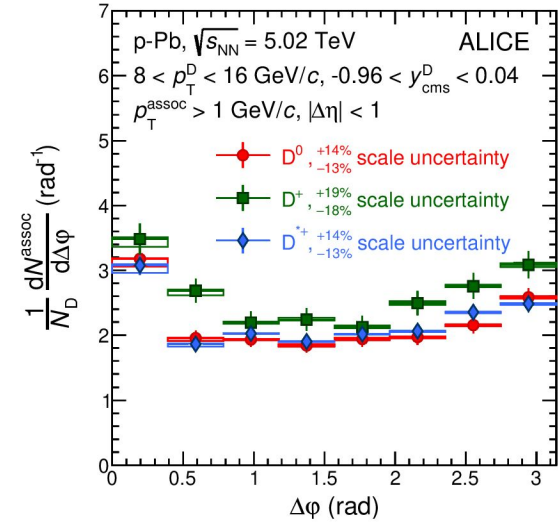
ALI-PREL-510407

- D^0 -meson $3 < p_T < 36$ GeV/c
- Charged jets, anti- k_T algorithm with $R = 0.3$
- Jet $5 < p_T < 50$ GeV/c

Comparison of correlation distributions in pp and p-Pb collisions

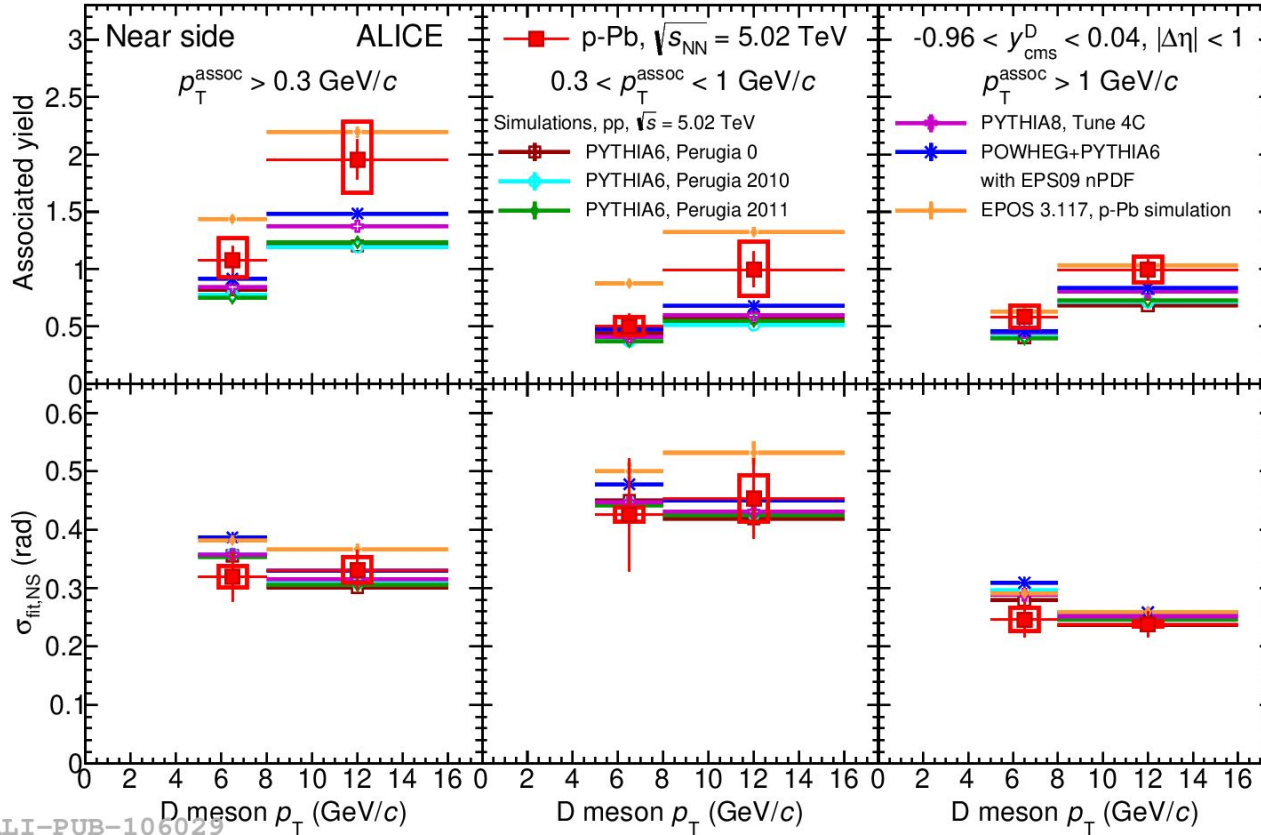


[EPJC 77 \(2017\) 245](#)

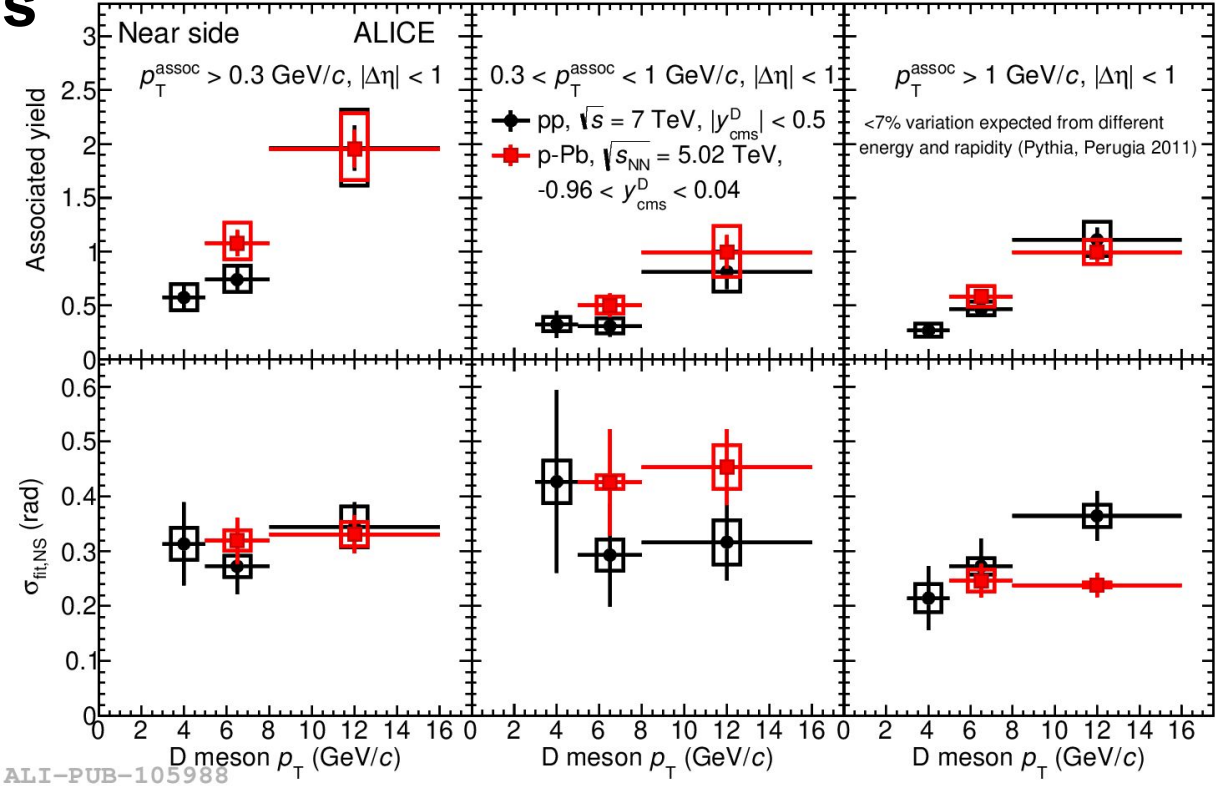


Near-side yield and widths in p–Pb collisions at 5.02 TeV

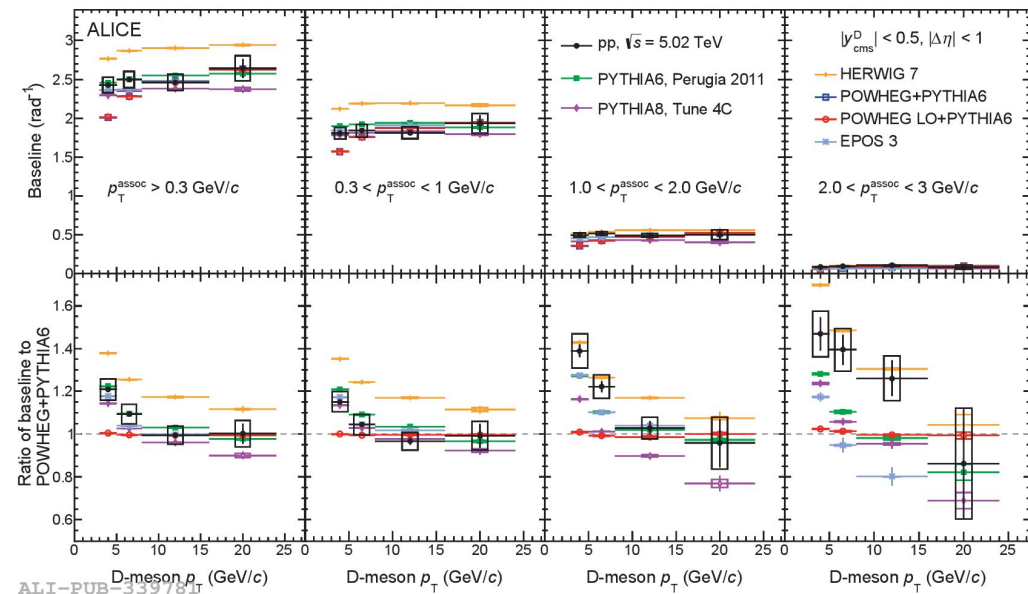
[EPJC 80 \(2020\) 979](#)



Comparison of near-side observables in pp and p-Pb collisions



D-meson Baseline comparison with models in pp at 5.02 TeV



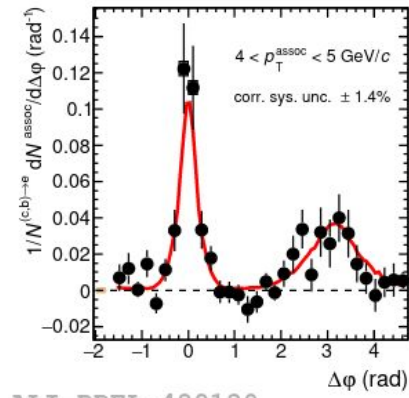
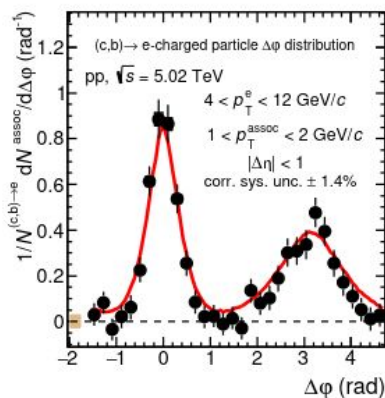
ALI-PUB-33978

[EPJC 80 \(2020\) 979](#)

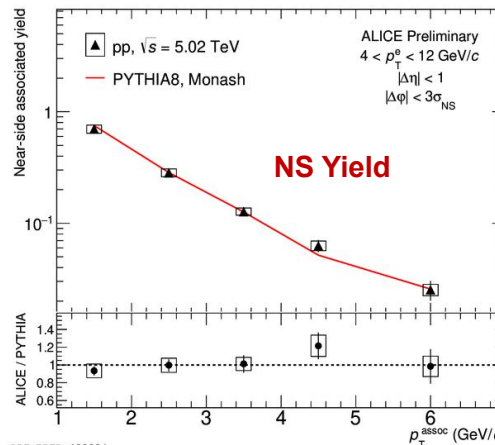
HFe-charged particles azimuthal correlation distributions



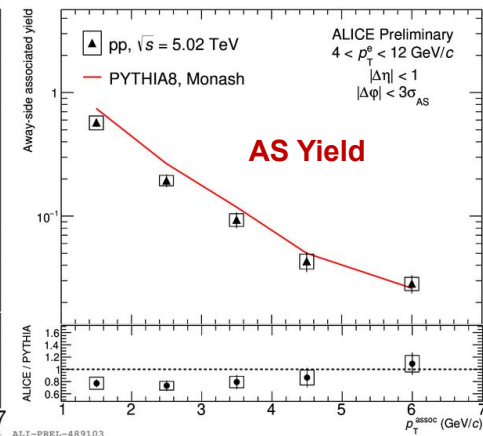
ALICE



ALI-PREL-489120



ALI-PREL-489824



ALI-PREL-489103

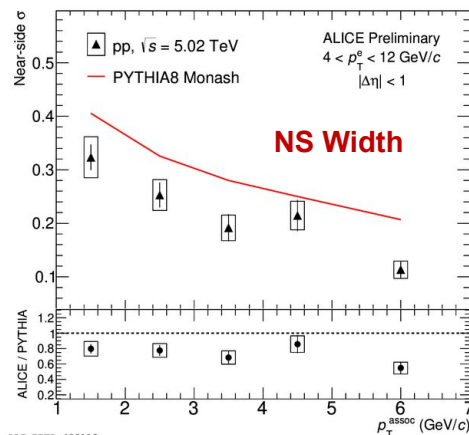
HF-electron sources are:

- semi-electronic decays of heavy-flavour hadrons.

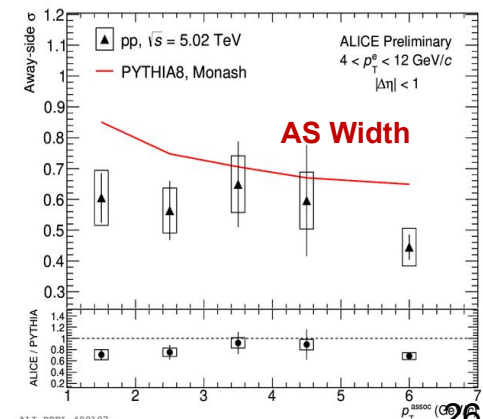
Main background contributions come from:

- Dalitz decays of light neutral mesons.
- Photon conversion in the detector material.
- The azimuthal correlation distribution undergoes a correction procedure similar to that of the D-meson distribution.
- Fitting procedure is same as in D-meson.

- NS yield is very well reproduced by the PYTHIA8.
- Both the widths are underestimated by the PYTHIA8 predictions.

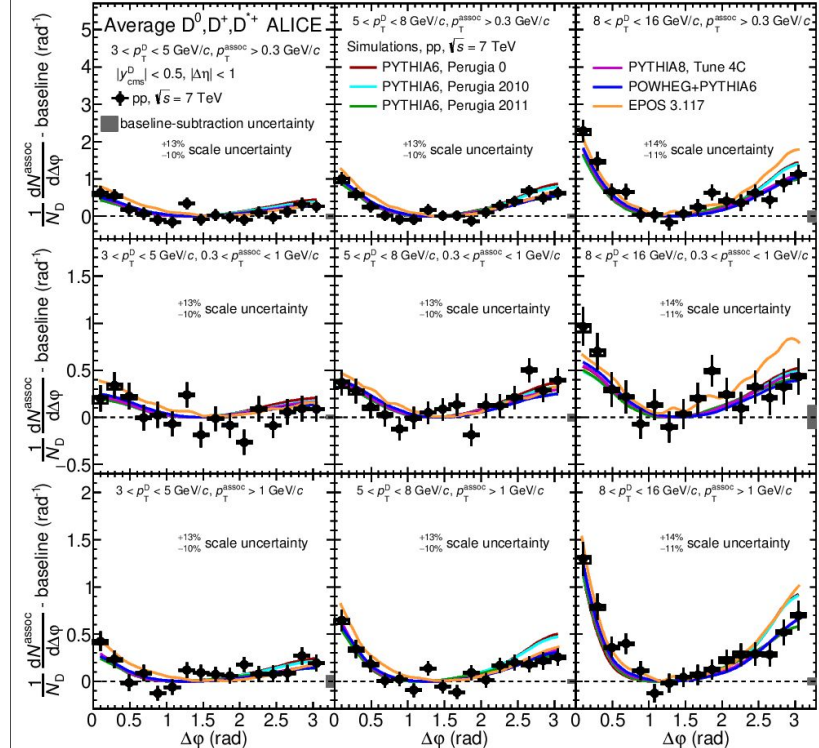
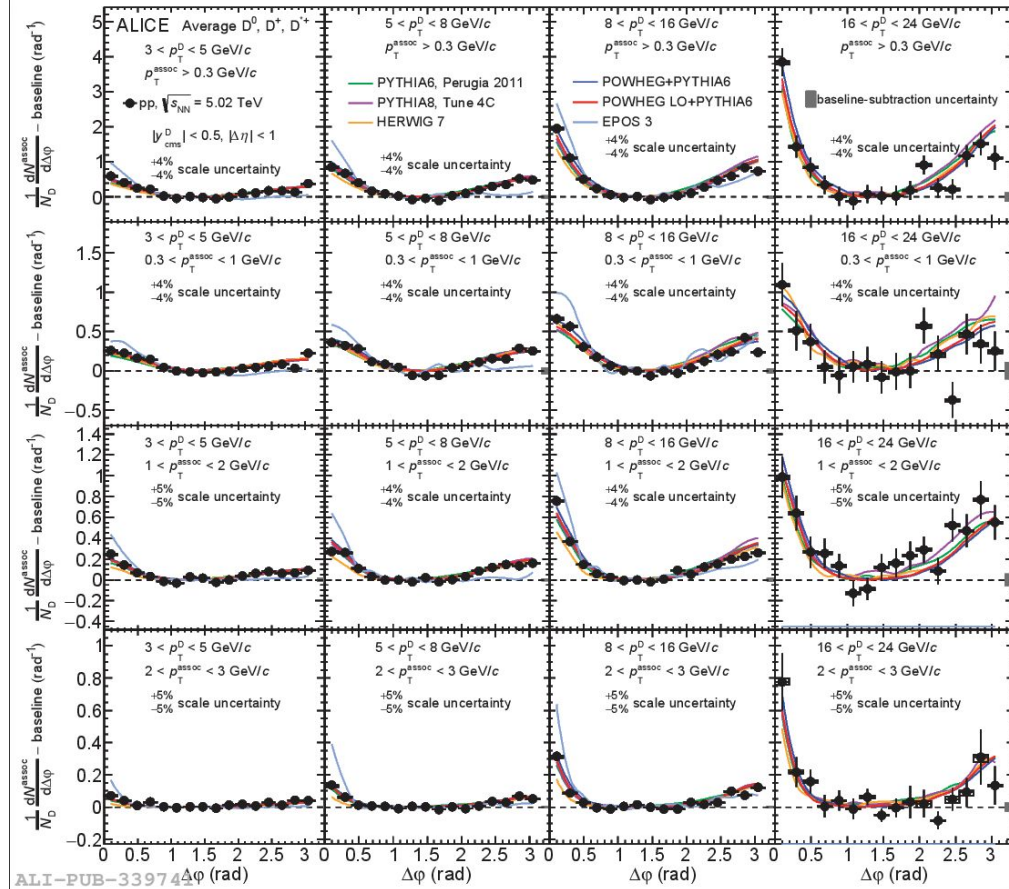


ALI-PREL-489112



ALI-PREL-489107

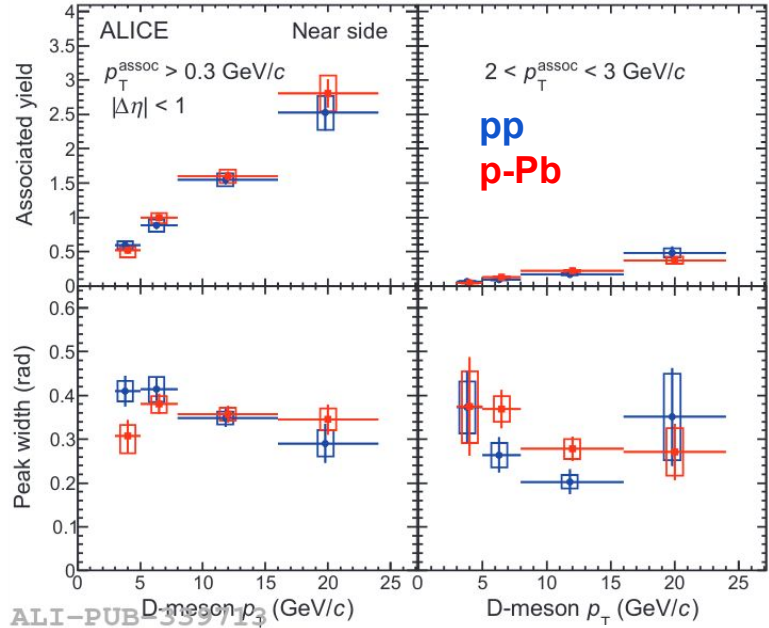
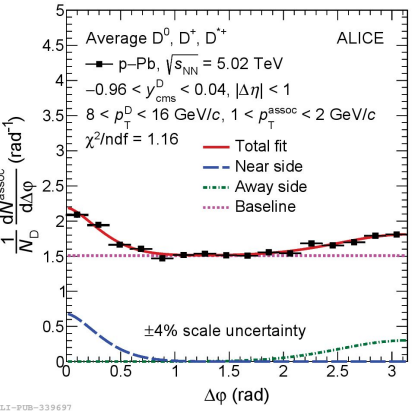
Model comparisons of D-charged particle correlation distribution in at 5.02 and 7 TeV





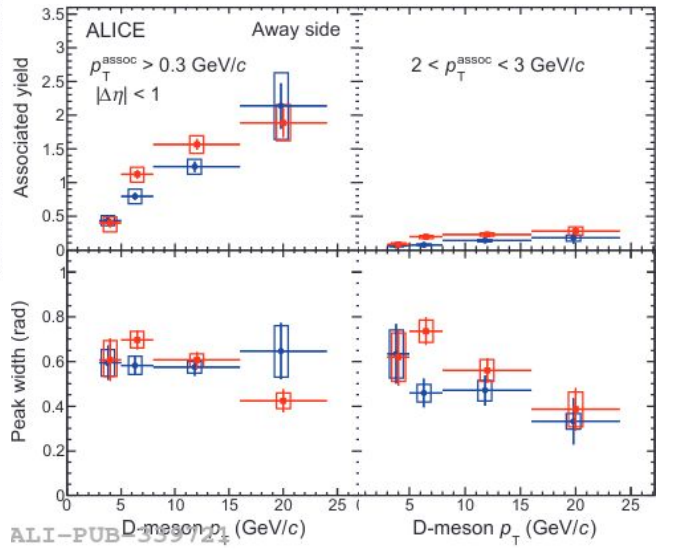
ALICE

D-meson and charged particle azimuthal correlation



- Consistent values of the fit observables in pp and p-Pb collisions are observed in all kinematic ranges.
- no significant impact from cold-nuclear-matter effects on the charm fragmentation is observed with current statistics.

ALI-PUB-3397/13
 EPJC 80 (2020) 979



ALI-PUB-3397/14

Fitting procedure:

- constant term (Baseline) + Generalized Gaussian (Near-side) + Gaussian (Away-side)

$$f(\Delta\varphi) = b + \frac{Y_{NS} \times \beta}{2\alpha\Gamma(1/\beta)} \times e^{-\left(\frac{\Delta\varphi}{\alpha}\right)^\beta} + \frac{Y_{AS}}{\sqrt{2\pi}\sigma_{AS}} \times e^{-\frac{(\Delta\varphi-\pi)^2}{2\sigma_{AS}^2}}$$



HFe-charged particles azimuthal correlation distributions

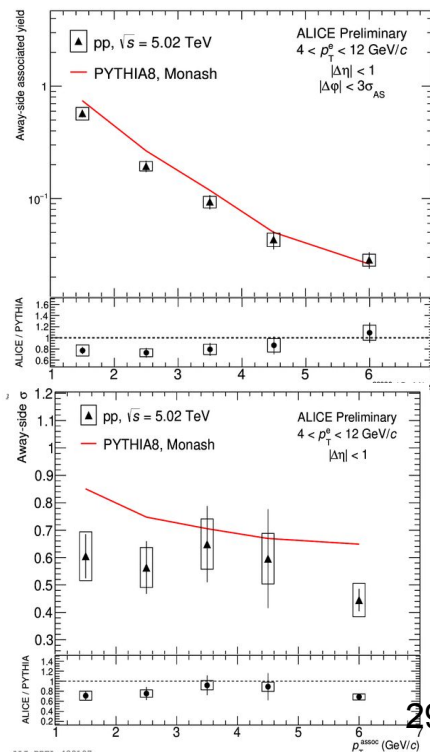
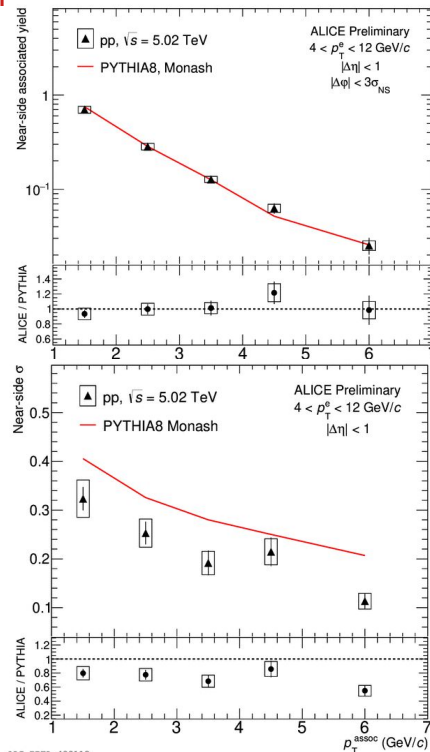
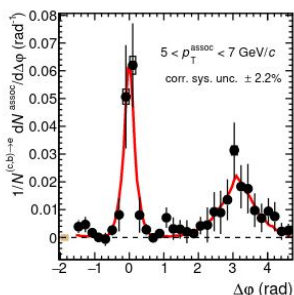
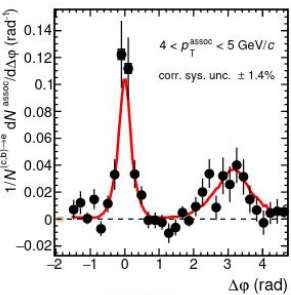
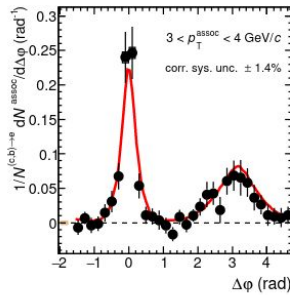
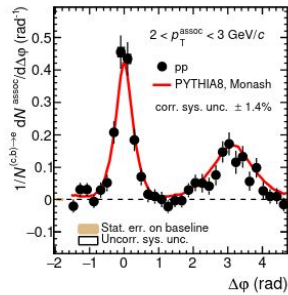
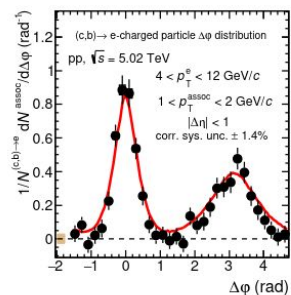
HF-electron sources are:

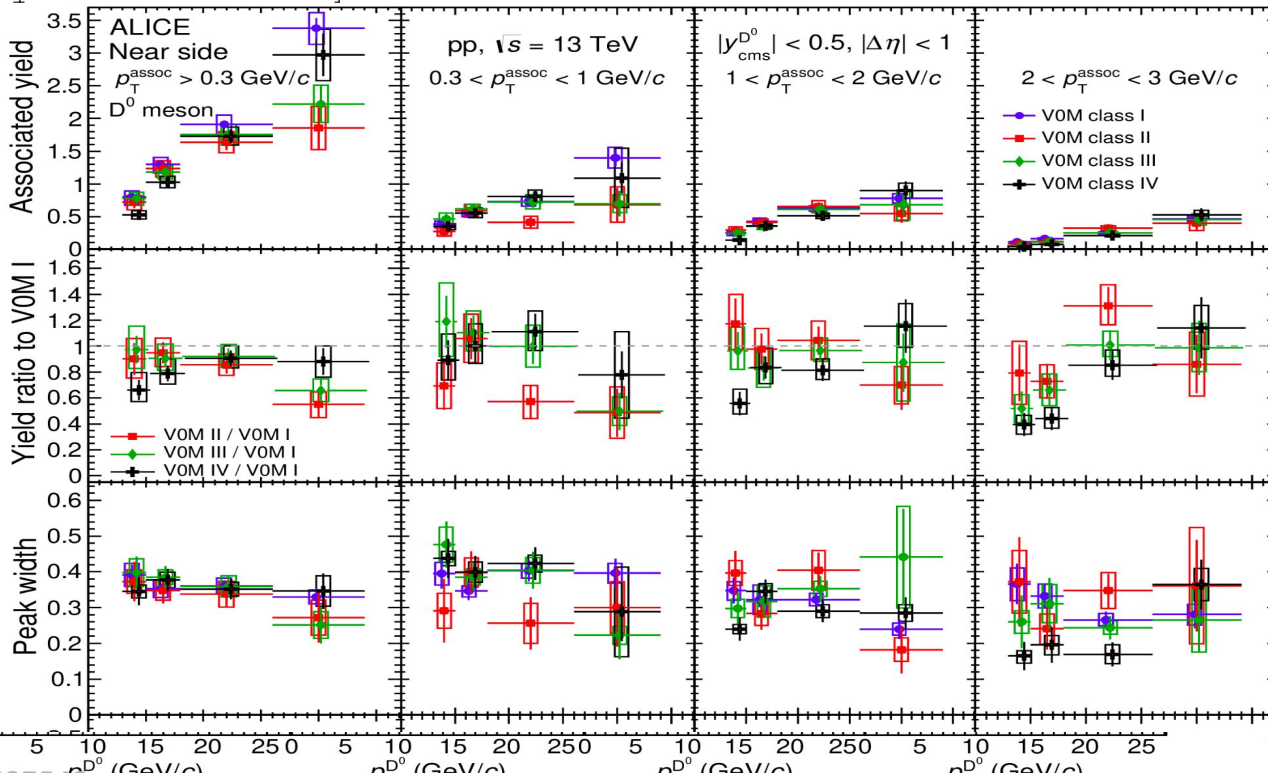
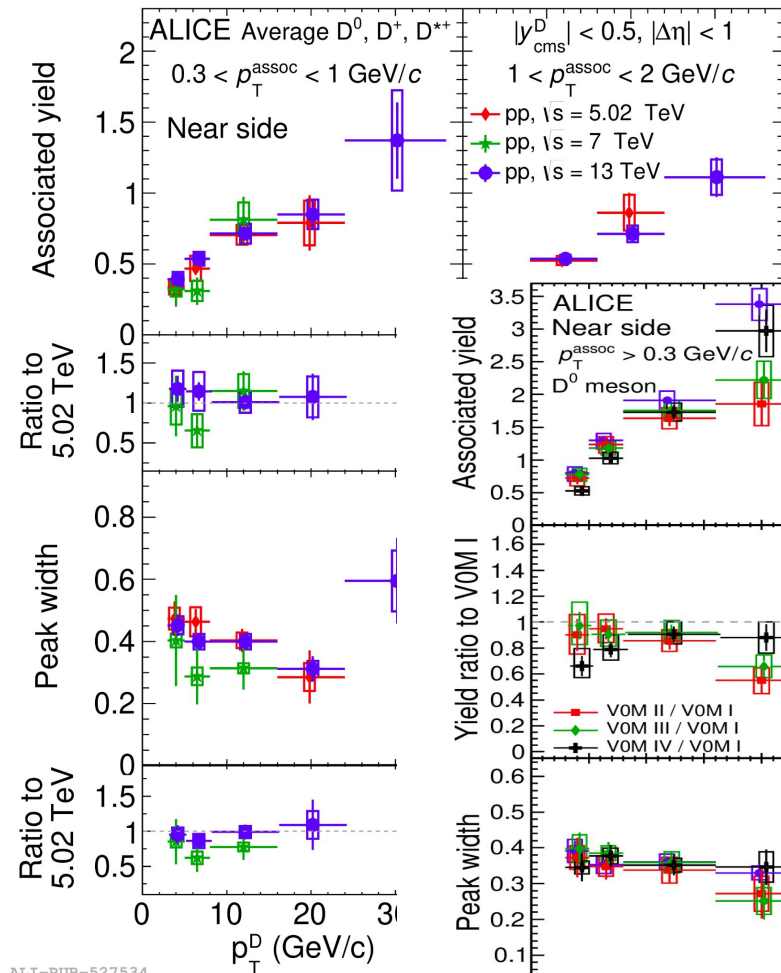
- semi-electronic decays of heavy-flavour hadrons.

Main background contributions come from:

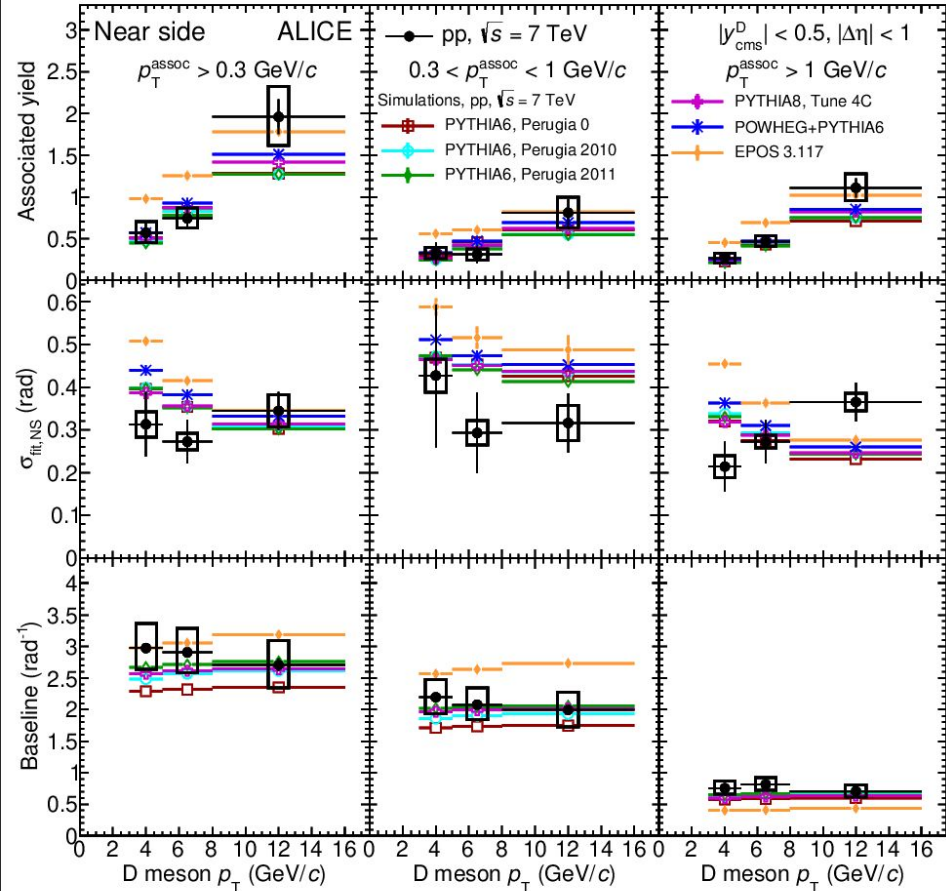
- Dalitz decays of light neutral mesons.
- Photon conversion in the detector material.
- The azimuthal correlation distribution undergoes a correction procedure similar to that of the D-meson distribution.
- Fitting procedure is same as in D-meson.

- NS yield is very well reproduced by the PYTHIA8.
- Both the widths are underestimated by the PYTHIA8 predictions.





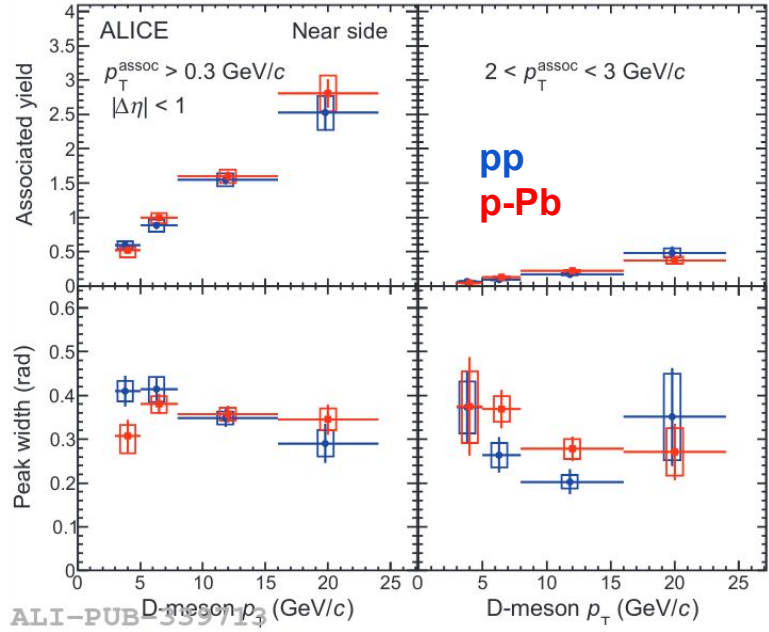
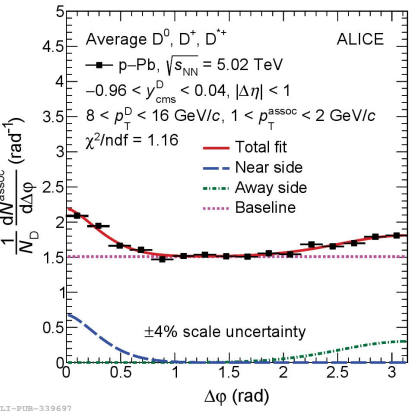
Near-side observables and baseline in pp collisions at 7 TeV





ALICE

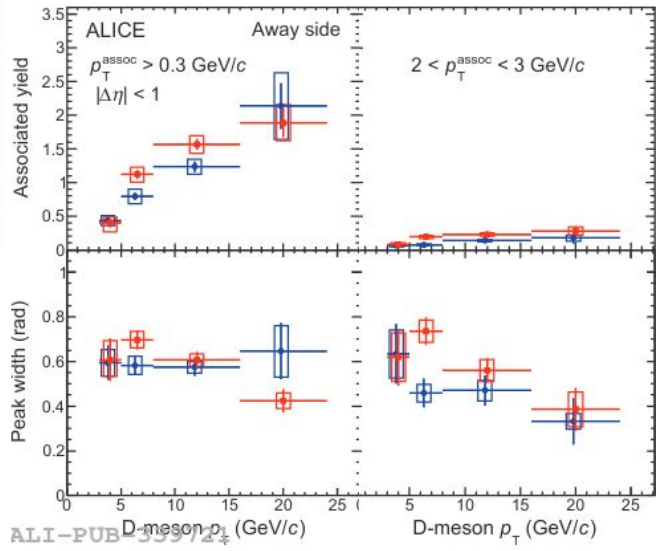
D-meson and charged particle azimuthal correlation



- Consistent values of the fit observables in pp and p-Pb collisions are observed in all kinematic ranges.
- no significant impact from cold-nuclear-matter effects on the charm fragmentation is observed with current statistics.

ALI-PUB-3399/13

[EPJC 80 \(2020\) 979](#)



ALI-PUB-3399/14

Fitting procedure:

- constant term (Baseline) + Generalized Gaussian (Near-side) + Gaussian (Away-side)

$$f(\Delta\varphi) = b + \frac{Y_{NS} \times \beta}{2\alpha\Gamma(1/\beta)} \times e^{-\left(\frac{\Delta\varphi}{\alpha}\right)^\beta} + \frac{Y_{AS}}{\sqrt{2\pi}\sigma_{AS}} \times e^{-\frac{(\Delta\varphi-\pi)^2}{2\sigma_{AS}^2}}$$

D-meson and charged particle azimuthal correlation

Comparison among partonic processes with PYTHIA8 and POWHEG+PYTHIA8

